

1

Arizona Aquifer Recharge Suitability Analysis

2

Travis Zalesky¹

3

¹University of Arizona,

Corresponding author: Travis Zalesky, travisz@arizona.edu

Abstract

Aquifer recharge can be either passive or active, and is implemented in a variety of ways. This analysis seeks to identify regions across AZ which are broadly suitable for aquifer recharge projects as a general template for more focused analysis.

Plain Language Summary

Identifying regions in AZ where surface water can be stored long-term as ground water.

0.1 Introduction

0.2 Data & Methods

These methods and data layers are preliminary and subject to change

0.2.1 Elevation

0.2.1.1 DEM

Elevation and elevation derivatives from 30-m NASA SRTM. USGS 3-DEM (10m) product not suitable for full study area analysis due to (1) the large area of missing data in Mexico, and (2), the excessively high spatial resolution (massively increasing computational requirements).

SRTM elevation sinks filled prior to calculating slope and aspect.

Should elevation be directly used in the suitability analysis?

0.2.1.2 Slope

Slope derived from hydrologically conditioned (filled) 30-m SRTM layer using quadratic surface function and a fixed 30-m neighborhood. Slope measured in $^{\circ}$.

Higher slopes are less suitable because thinning is both more expensive and more precipitation will end up as runoff.

Slope classified from 1-10 using a **continuous function** in ArcPro Suitability Mapper.

Pamameter	Setting
Function	MSSSmall
Mean multiplier	1
Sddv multiplier	2
Lower threshold	0
Value below threshold	0
Upper threshold	90
Value above threshold	0
Invert function	FALSE
Save transformed dataset	TRUE
Output	Transformed_SRTM_slope

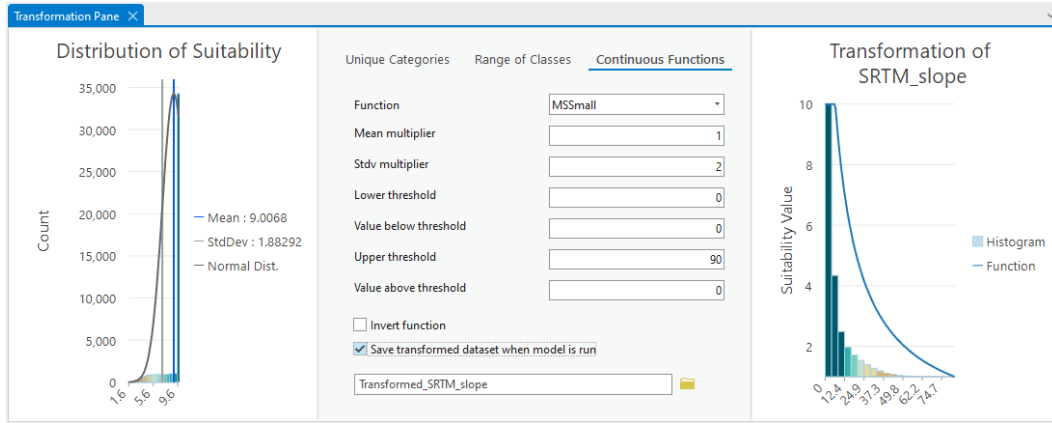


Figure 1: Slope suitability mapper rescale transformation setup.

0.2.1.3 Aspect

Aspect calculated as with slope. Aspect reference point at N. Pole.

Aspect has a large impact on solar radiation.

Closer to 0 or 360 is desired, low suitability scores for closeness.

Aspect classified from 1-10 using a **continuous function** in ArcPro Suitability Mapper.

Pamameter	Setting
Function	Near
Mid Point	180
Point spread	0.0011049638968393428 (default)
Lower threshold	-1 (flat)
Value below threshold	0
Upper threshold	360
Value above threshold	0
Invert function	TRUE
Save transformed dataset	TRUE
Output	Transformed_SRTM_aspect

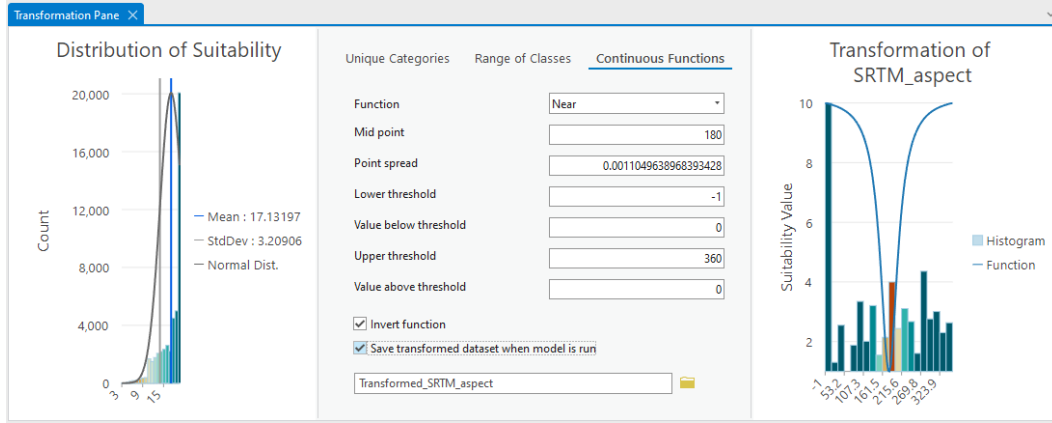


Figure 2: Aspect suitability mapper rescale transformation setup.

0.2.2 Precipitation

PRISM normals, 800m resolution. Annual precipitation.

Mean annual precipitation must be higher than 500mm 1990 - 2020

Precipitation classified from 1-10 using a **continuous function** in ArcPro Suitability Mapper.

NOTE: The logistic growth function may also be a good choice for this dataset. See [Logistic Growth function](#)

Pamameter	Setting
Function	MSLarge
Mean multiplier	1.68 (aproximates 500mm at x-intercept)
Sddv multiplier	1
Lower threshold	67.33789825439453 (default, minimum)
Value below threshold	0
Upper threshold	1214.5689697265625 (default, maximum)
Value above threshold	0
Invert function	FALSE
Save transformed dataset	TRUE
Output	Transformed_PRISM_ppt_30yrnormal_800m

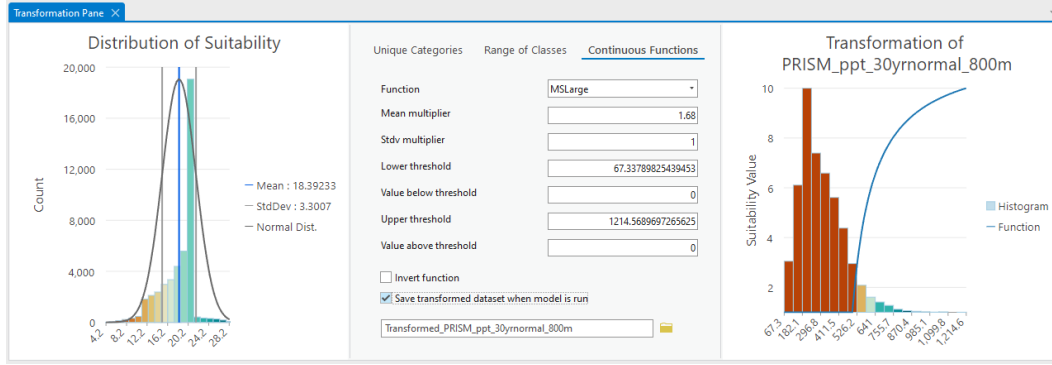


Figure 3: Aspect suitability mapper rescale transformation setup.

0.2.3 Vegetation Characteristics

0.2.3.1 NLCD 2021 Total Canopy Cover

0.2.3.2 Landfire

0.2.4 Soil Hydrology

AZ_Soil_Hydric_Group data layer

Classification Schema

Class	Count (pixels)	Text	Value
A	62559472	Group A soils consist of deep, well drained sands or gravelly sands with high infiltration and low runoff rates.	10
B	76665198	Group B soils consist of deep well drained soils with a moderately fine to moderately coarse texture and a moderate rate of infiltration and runoff.	8
C	88491710	Group C consists of soils with a layer that impedes the downward movement of water or fine textured soils and a slow rate of infiltration.	5
D	155095790	Group D consists of soils with a very slow infiltration rate and high runoff potential. This group is composed of clays that have a high shrink-swell potential, soils with a high water table, soils that have a clay pan or clay layer at or near the surface, and soils that are shallow over nearly impervious material.	2
A/D	43192	Group A/D soils naturally have a very slow infiltration rate due to a high water table but will have high infiltration and low runoff rates if drained.	7
B/D	18456	Group B/D soils naturally have a very slow infiltration rate due to a high water table but will have a moderate rate of infiltration and runoff if drained.	6

Class	Count (pixels)	Text	Value
C/D	217771	Group C/D soils naturally have a very slow infiltration rate due to a high water table but will have a slow rate of infiltration if drained.	3

Transformed dataset Transformed_AZ_Soil_Hydric_Group

0.2.5 Depth to Bedrock

There are 2 data layers which represent depth to bedrock and it is not clear which data layer is preferred!

- AZ_BedrockDepth_cm.tif
 - 218 m resolution
 - UTM 12N, NAVD88 depth (m) possitive down
 - 0 – 108,273 cm

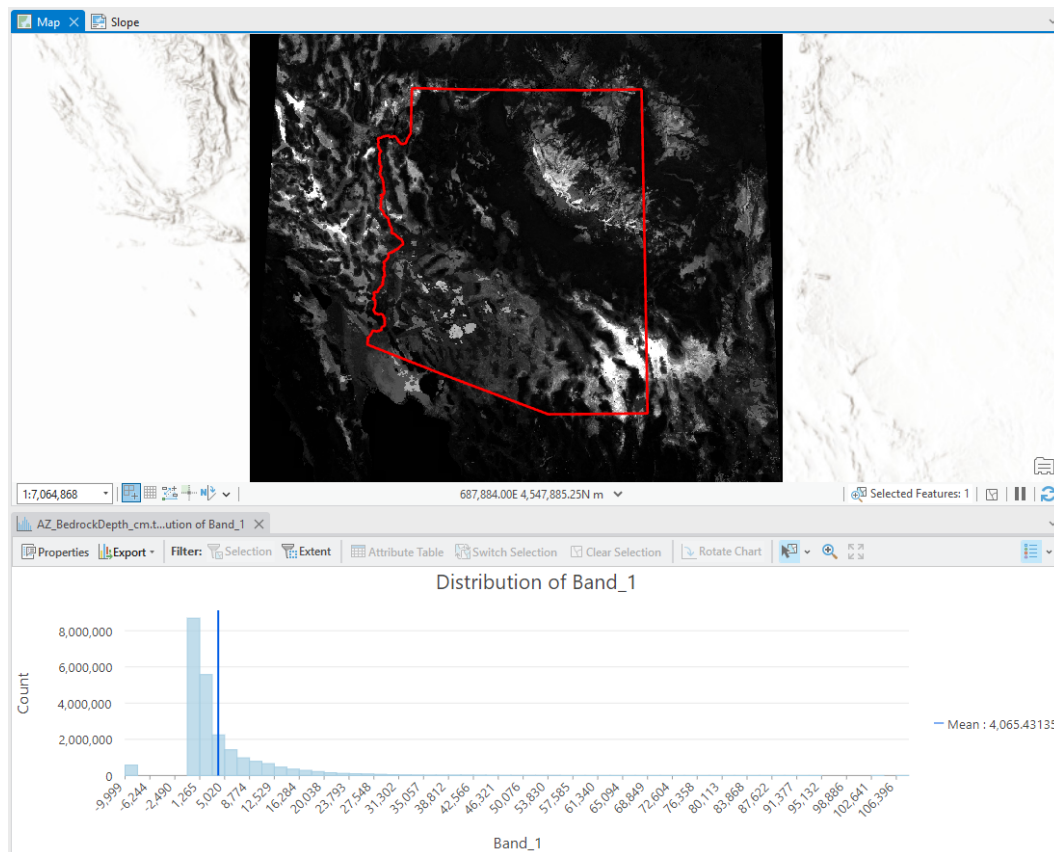


Figure 4: AZ_BedrockDepth_cm.tif with histogram.

- Depth to Bedrock WTA
 - Classified
 - 30 m resolution
 - UTM 12N, NAVD88 height (m) possitive up
 - * vertical datum is incorrect. Should be depth (m) possitive down

- 61 – 0 – 269 cm
- 62 – Extremely skewed distribution clustering around 200 cm

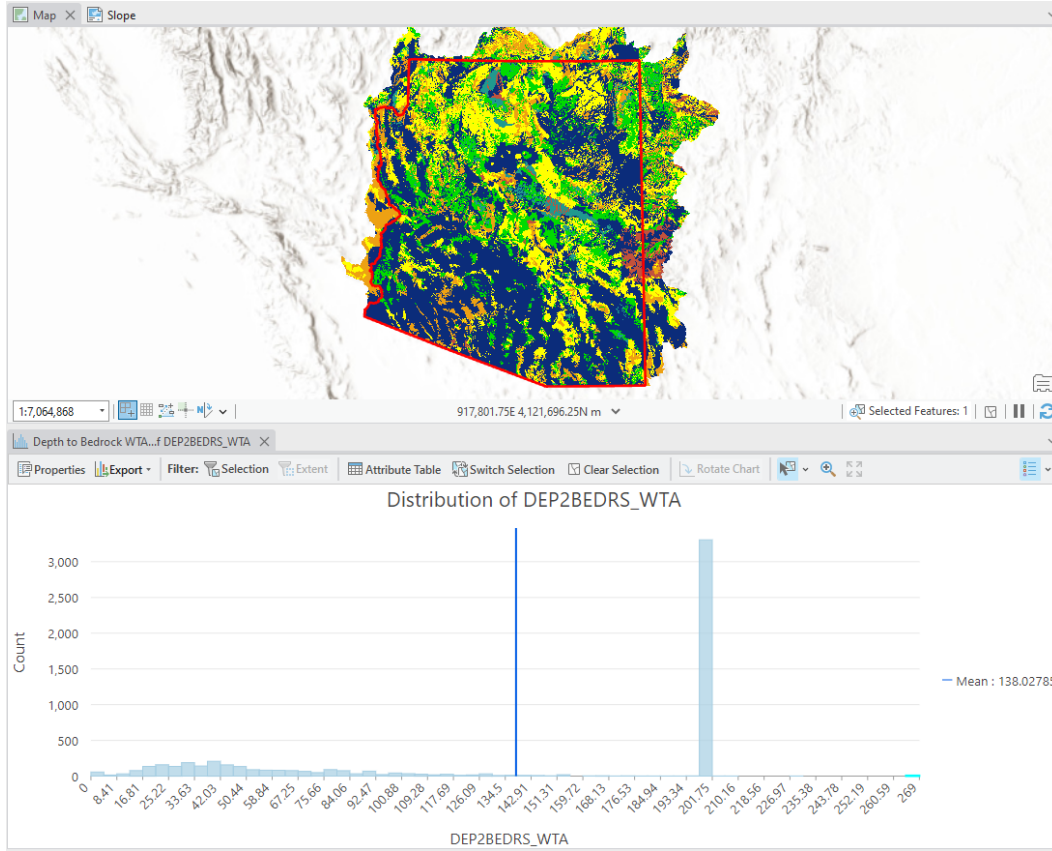


Figure 5: Depth to Bedrock WTA, DEP2BEDRS_WTA layer with histogram

63 0.2.5.1 Soil vs. Subsurface Geology Weighting Layers

64 To quantify the differential importance of soils vs. subsurface geology layers for deter-
 65 mining suitability two related data layers had to be calculated.

66 The logic assumes that there are two uniform subsurface layers, soil, and subsur-
 67 face geology (i.e. geology). However, the weighted importance of these layers is not
 68 uniform across space. Where the bedrock is close to the surface, we assume that
 69 the soil is the most important layer for ground water storage. Inversely, when the
 70 bedrock is extremely deep, we assume that the geology is the more important layer.
 71 Our soil layer is measured at a depth of 200cm (2m), and we assume a uniform soil
 72 depth across the state. Therefore, the depth to bedrock was divided by 200 to get a
 73 depth to bedrock (dtb) in soil units. The first “soil depth” was ascribed to the soil
 74 layer, and varies from 0 to 1, while the remaining “soil depth” were attributed to the
 75 geology layer, with a range from 0 to 541. Ergo, where the bedrock is deepest, the
 76 geology layer is 541 time more influential than the soils layer.

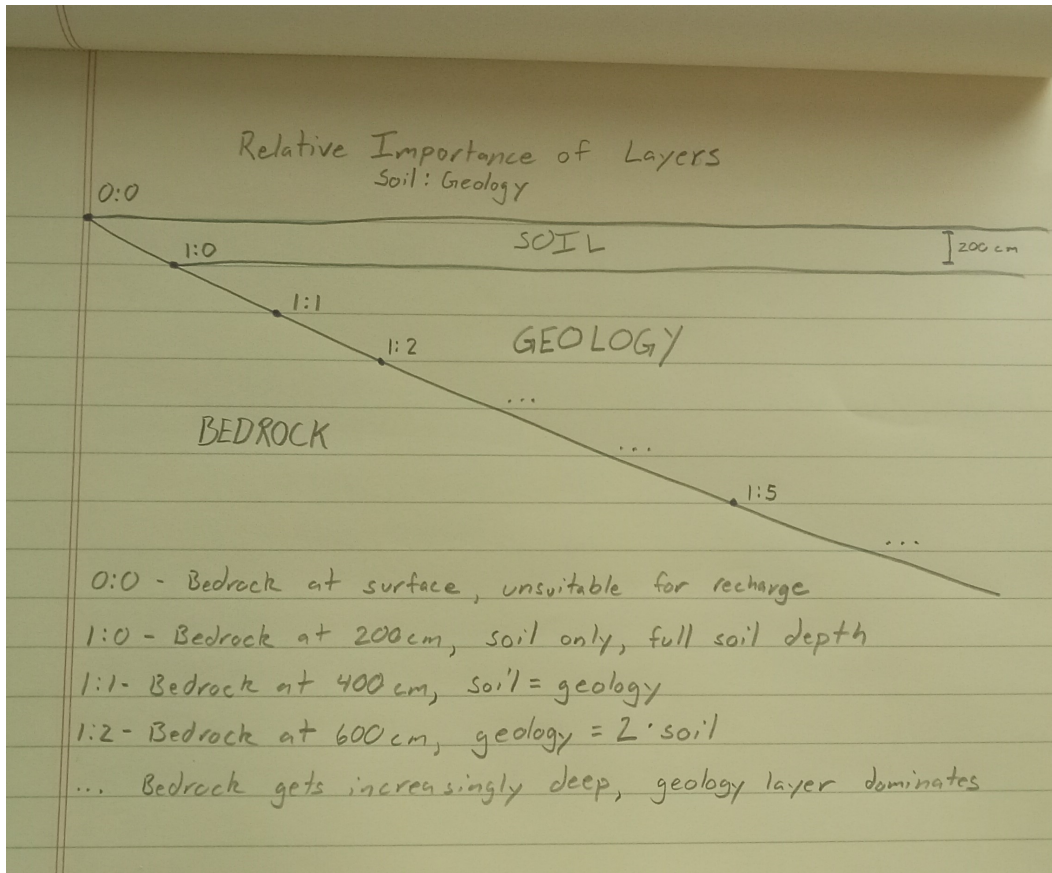


Figure 6: Simple diagram of logic underlying the soil vs. subsurface geology weighting layers.

These layers were created in a custom R script using the following raster math, with their resulting outputs.

0.2.5.1.1 Soils

```
```{r}
Where depth to bedrock (dtb) = 0cm, soil multiplier = 0 (no soil)
Where depth to dtb >= 200cm, soil multiplier = 1 (Full depth of soil)
Intermediate depths = linear
soilMultiplier = masked
soilMultiplier[soilMultiplier > 200] = 200 # Fix upper limit of soil depth = 200 cm
soilMultiplier = soilMultiplier/200
```
```

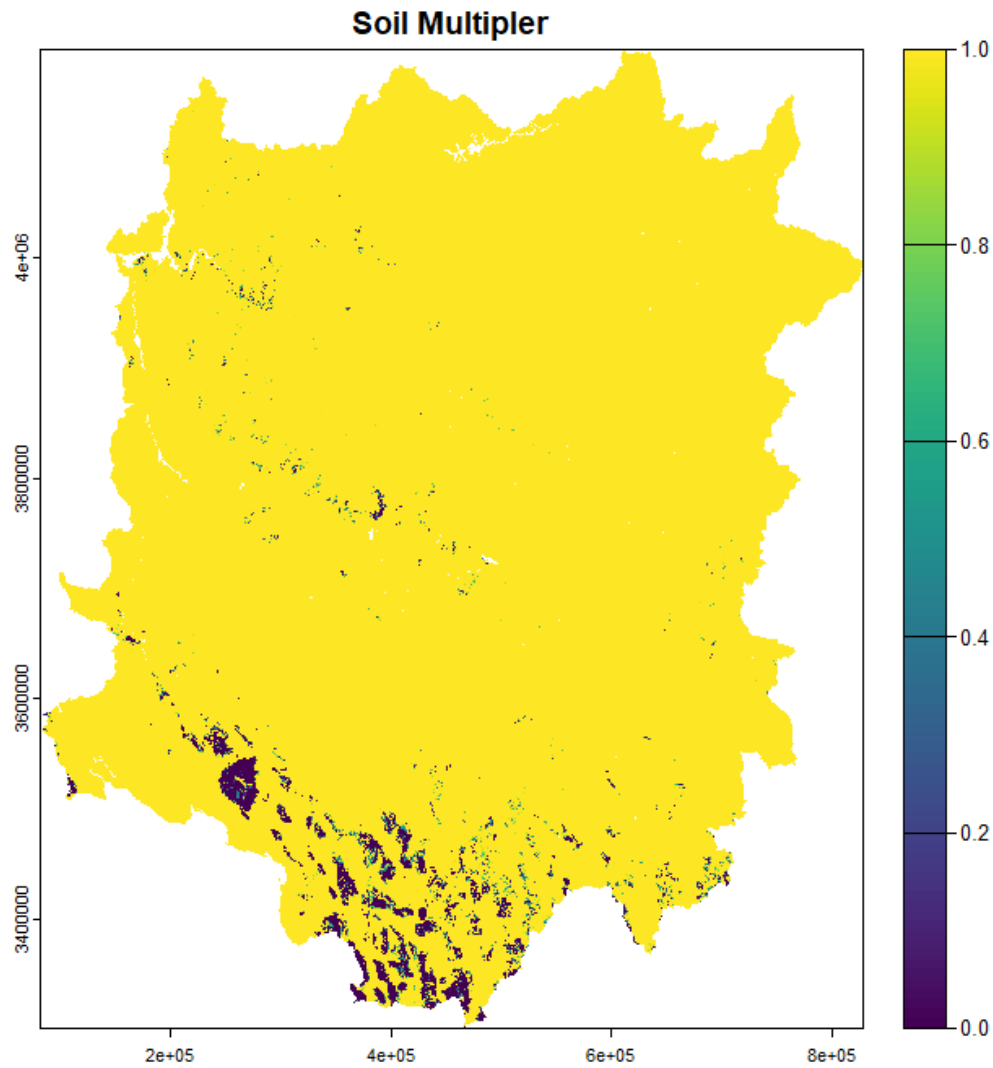



Figure 7: Soils multiplier layer.

80

0.2.5.1.2 Geology

```

```{r}
Where dtb < 200cm, geology multiplier = 0 (soil only)
Where dtb >= 200cm, geology multiplier = dtb/200 (in units of relative soil depth)
geologyMultiplier = masked
geologyMultiplier[geologyMultiplier < 200] = 0
geologyMultiplier = geologyMultiplier/200
```

```

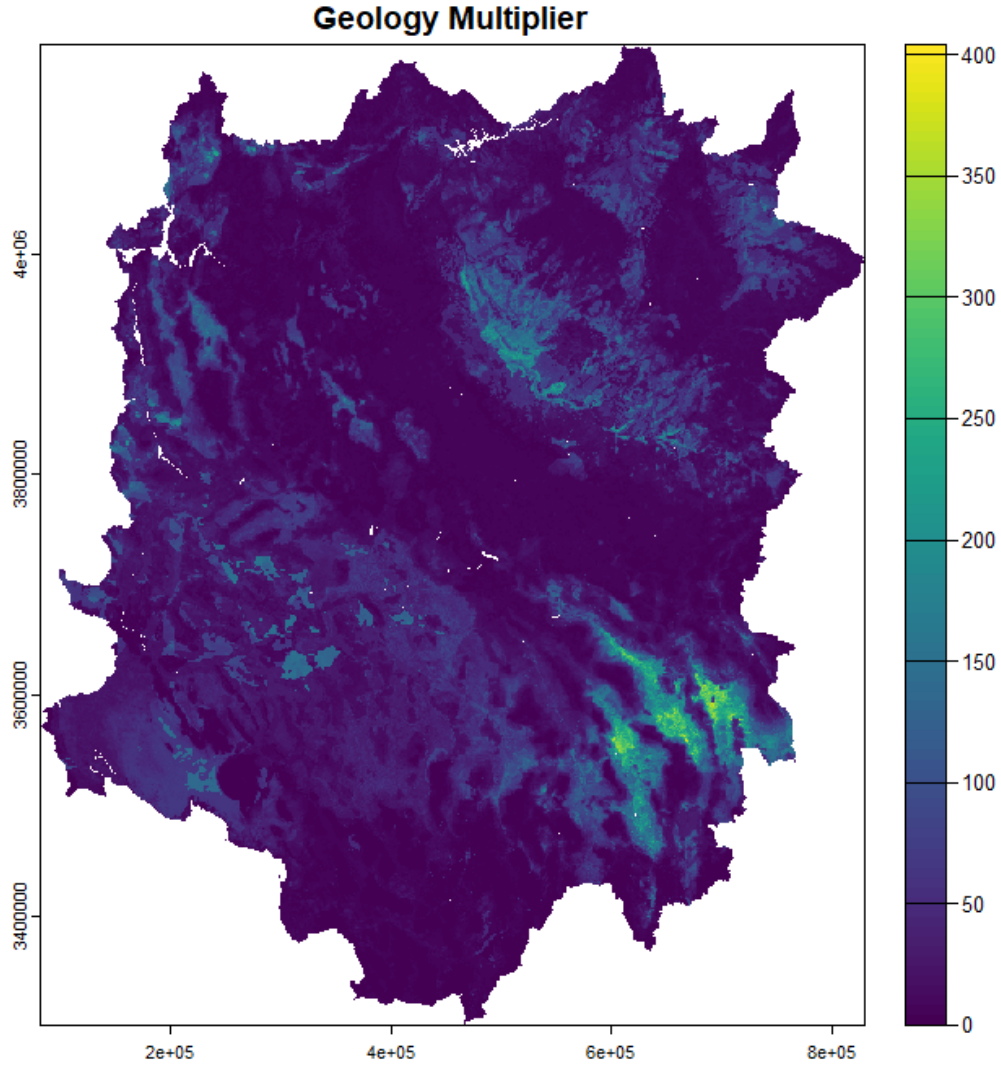


Figure 8: Geology multiplier layer.

0.2.6 Other Data Layers for Consideration

0.2.6.1 Global Hydrologic Curve Number(GCN250)

<https://gee-community-catalog.org/projects/gcn250/?h=hydrologic>

The GCN250 is a globally consistent, gridded dataset defining CNs at the **250 m spatial resolution** from new global land cover (300 m) and soils data (250 m). GCN250 **represents runoff** for a combination of the European space agency global land cover dataset for 2015 (ESA CCI-LC) resampled to 250 m and geo-registered with the hydrologic soil group global data product (HYSOGs250m) released in 2018. The **potential application** of this data includes **hydrologic design**, land management applications, flood risk assessment, and **groundwater recharge modeling**. The CN values vary depending on antecedent runoff conditions (ARC), which is affected by the

rainfall intensity and duration, total rainfall, soil moisture conditions, cover density, stage of growth, and temperature[.] *emphasis mine*

0.2.6.2 Soil Properties 800m

<https://gee-community-catalog.org/projects/soilprop/?h=>

The data shown here were obtained by aggregating current USDA-NCSS soil survey data (SSURGO back-filled with STATSGO where SSURGO is not available) within **800m² grid cells**. This data aggregation technique results in maps that may not match the original data at any given point, and is **intended to depict regional trends in soil properties at the statewide scale**. *emphasis mine*

- Pros:
 - Lots of relevant data layers, such as:
 - * Avail. Water Holding Capacity
 - * Drainage Class
 - * Sat. Hyd. Conductivity
 - * Depth to Restrictive Layer
 - * Hydrologic Group
 - * Soil Depth
 - * etc.
- Cons:
 - 800m resolution
 - Large data gaps (layer dependent)

0.2.6.2.1 Alternative layers

[gNATSGO \(gridded National Soil Survey Geographic Database\)](#)

- Pros:
 - Authoritative
 - Source layer for value added products (including Soil Properties 800m)
 - 10m resolution
- Cons:
 - Large data gaps across AZ
 - 10m resolution

[Polaris 30m Probabilistic Soil Properties US](#)

- Pros:
 - Continuous data availability (no gaps)
 - 30m resolution
- Cons:
 - Fewer data layers
 - Probabalistic model (increased uncertainty)

0.2.6.3 Leaf Area Index (LAI)

Leaf Area Index (LAI) can be calculated from Landsat data (30 m resolution), as a proxy of landcover. LAI is a unitless index value which is calculated as a function of the Enhanced Vegetation Index (ENVI) and typically ranges from 0 to 3.5 (*citation needed*). LAI can be calculated effincintly over a large spatial scale in Google Earth Engine (GEE) using the Javascript API, however LAI will vary seasonally, with updated Landsat data available every 8-days. Additionally, due to our large study area, as well as the logistics of Landsat orbital paths, it takes 6 days to photograph the entier study area. Therefore, any LAI analysis on this scale will necessaraly be a mosaic image, over roughly a week. For these reasons, a single LAI image should be

viewed with some skepticism, and a seasonal mean or median LAI mosaic image may be more desirable as a proxy for landcover.

Code is available for calculating LAI from Landsat 8/9 imagery in my personal GEE scripts folder, which could be easily modified for purpose. Due to the large number of Landsat images involved the study period must be narrowed prior to analysis (i.e. July LAI, Winter LAI, etc.). Additional post-processing of LAI images may be required outside of GEE.

0.2.6.3.1 Google Earth Engine LAI Javascript Code

```
var studyArea = ee.FeatureCollection("projects/ee-travisz09/assets/ATUR/WBDHU8_OuterBoundary_Pr
landsat9 = ee.ImageCollection("LANDSAT/LC09/C02/T1_TOA");

// Map setup
Map.centerObject(studyArea, 6);
Map.addLayer(studyArea, {}, 'Study Area', false);

// Paint study area outline
var empty = ee.Image().byte(); // An empty layer to paint on
var studyAreaOutline = empty.paint(studyArea, 'black', 2);
Map.addLayer(studyAreaOutline, {}, 'Study Area (outline)');

// Study period
var startDate = ee.Date('2023-01-01');
var endDate = ee.Date('2024-01-01'); // Exclusive end date
var timeDif = endDate.difference(startDate, 'day');
// var interval = 8; // days
// print(timeDif);

// Landsat 8/9
var cloudFilter = 10 // 10% max cloud cover
var landsat = ee.ImageCollection('LANDSAT/LC08/C02/T1_L2')
  .merge(ee.ImageCollection('LANDSAT/LC09/C02/T1_L2')) // Combine Lst-9 and Lst-8
  .filterDate(startDate, endDate)
  .filterBounds(studyArea)
  .sort('system:time_start') // Sort by date
  .filter(ee.Filter.lt('CLOUD_COVER', cloudFilter));

// Lst scaling factor function
var scaleLst = function(col) {
  // Map over images in collection
  var scaled = col.map(function(img) {
    var opticalBands = img.select('SR_B.').multiply(0.0000275).add(-0.2);
    var thermalBands = img.select('ST_B.*').multiply(0.00341802).add(149.0);

    return img.addBands(opticalBands, null, true) // Overwrite unscaled bands
      .addBands(thermalBands, null, true);
  });

  return scaled;
};

// print(landsat.first()); // Check the Lst data before scaling
landsat = scaleLst(landsat); // Apply scaling factor
// print(landsat.first()); // Check Lst data after scaling
```

```

// NDVI, EVI, LAI, index function
var calcIndices = function(col) {
  var indices = col.map(function(img) {
    var ndvi = img.normalizedDifference(['SR_B5', 'SR_B4'])
      .rename('ndvi');
    var evi = img.expression(
      '2.5 * ((nir - red) / (nir + 6 * red - 7.5 * blue + 1))',
      {
        'nir': img.select('SR_B5'),
        'red': img.select('SR_B4'),
        'blue': img.select('SR_B2')
      }).rename('evi');
    var lai = evi.expression(
      '3.618 * evi - 0.118',
      {
        'evi': evi.select('evi')
      }).rename('lai');

    return img.addBands(ndvi)
      .addBands(evi)
      .addBands(lai);
  });

  return indices;
};

// Apply indices
landsat = calcIndices(landsat);
// print(landsat.first()); // sanity check

// Isolate lai bands
var lai = landsat.map(function(img) {
  return img.select('lai');
});

Map.addLayer(lai.limit(20), {
  min: 0,
  max: 3.5,
  palette: ['red', 'white', 'green']
}, 'LAI');
print(lai);

```

149

0.3 Conclusion

150

References